

**1 Microenvironmental variables must influence intrinsic  
2 phenotypic parameters of cancer stem cells to affect  
3 tumourigenicity**

**4** Jacob G. Scott<sup>1,2</sup>, Anita B. Hjelmeland<sup>3</sup>, Prakash Chinnaiyan<sup>4</sup>, Alexander R. A. Anderson<sup>1</sup>, David  
**5** Basanta<sup>1,\*</sup>

**6** **1 Integrated Mathematical Oncology, H. Lee Moffitt Cancer Center and Research  
7 Institute, Tampa, FL, USA**

**8** **2 Wolfson Centre for Mathematical Biology, Mathematical Institute, University of  
9 Oxford, Oxford, UK**

**10** **3 Department of Cell, Developmental and Integrative Biology, University of Alabama at  
11 Birmingham, Birmingham, AL, USA**

**12** **3 Department of Radiation Oncology, H. Lee Moffitt Cancer Center and Research  
13 Institute, Tampa, FL, USA**

**14** \* E-mail: Corresponding: jacob.g.scott@gmail.com, david@CancerEvo.org

**15 Abstract**

**16** Since the discovery of tumour initiating cells (TICs) in solid tumours, studies focussing on their role in  
**17** cancer initiation and progression have abounded. The biological interrogation of these cells continues to  
**18** yield volumes of information on their pro-tumourigenic behaviour, but actionable generalised conclusions  
**19** have been scarce. Further, new information suggesting a dependence of tumour composition and growth  
**20** on the microenvironment has yet to be studied theoretically. To address this point, we created a hybrid,  
**21** discrete/continuous computational cellular automaton model of a generalised stem-cell driven tissue with  
**22** a simple microenvironment. Using the model we explored the phenotypic traits inherent to the tumour  
**23** initiating cells and the effect of the microenvironment on tissue growth. We identify the regions in  
**24** phenotype parameter space where TICs are able to cause a disruption in homeostasis, leading to tissue  
**25** overgrowth and tumour maintenance. As our parameters and model are non-specific, they could apply  
**26** to any tissue TIC and do not assume specific genetic mutations. Targeting these phenotypic traits  
**27** could represent a generalizable therapeutic strategy across cancer types. Further, we find that the  
**28** microenvironmental variable does not strongly effect the outcomes, suggesting a need for direct feedback  
**29** from the microenvironment onto stem-cell behaviour in future modelling endeavours.

**30 Author Summary**

**31** In this paper, we present a mathematical/computational model of a tumour growing according to the  
**32** canonical cancer stem-cell hypothesis with a simplified microenvironment. We explore the parameters  
**33** of this model and find good agreement between our model and other theoretical models in terms of the  
**34** intrinsic cellular parameters, which are difficult to study biologically. We find, however, disagreement be-  
**35** tween novel biological data and our model in terms of the microenvironmental changes. We conclude that  
**36** future theoretical models of stem-cell driven tumours must include specific feedback from the microen-  
**37** vironment onto the individual cellular behavior. Further, we identify several cell intrinsic parameters  
**38** which govern loss of homeostasis into a state of uncontrolled growth.

## <sup>39</sup> Introduction

<sup>40</sup> Heterogeneity among cancer cells within the same patient contributes to tumour growth and evolution.  
<sup>41</sup> A subpopulation of tumour cells, called Tumour Initiating cells (TICs), or cancer stem cells, has recently  
<sup>42</sup> been shown to be highly tumourigenic in xenograft models and have some properties of normal stem  
<sup>43</sup> cells. Evidence continues to emerge that TICs can drive tumour growth and recurrence in many cancers,  
<sup>44</sup> including, but not limited to, brain [1], breast [2] and colon [3]. These tumour types can be broadly classed  
<sup>45</sup> as hierarchical as they have been posited to have a hierarchical organisation similar but not identical  
<sup>46</sup> to non-neoplastic stem-cell (SC) driven tissues. In these hierarchical tumors, TICs can differentiate  
<sup>47</sup> to produce non-TIC cancer cells or self-renew to promote tumor maintenance. As TICs have been  
<sup>48</sup> demonstrated to be resistant to a wide variety of therapies including radiation and chemotherapy, the  
<sup>49</sup> TIC hypothesis has important implications for patient treatments [4]. Specifically, the effect of current  
<sup>50</sup> strategies on the tumor cell hierarchy should be defined, and TIC specific therapies are likely to provide  
<sup>51</sup> strong benefit for cancer patients.

<sup>52</sup> In a simplified view of the tumour cell hierarchy, TICs can divide symmetrically or asymmetrically  
<sup>53</sup> to produce two TIC daughters or a TIC daughter and a more differentiated progeny [5, 6], respectively.  
<sup>54</sup> More differentiated TIC progeny which still have the capability of cell division and are similar to transient  
<sup>55</sup> amplifying cells (TACs) in the standard stem-cell model and are capable of several rounds of their own  
<sup>56</sup> symmetric division before the amplified population then differentiates into terminally differentiated cells  
<sup>57</sup> (TDs) which are incapable of further division. This mode of division and differentiation, which we will  
<sup>58</sup> call the Hierarchical Model (HM) is schematized in Figure 1.

<sup>59</sup> In the HM, there are a number of cellular behaviours that govern the system. In this study, we choose  
<sup>60</sup> to study three: the rate of symmetric versus asymmetric division of the stem cells ( $\alpha$ ), the number of  
<sup>61</sup> rounds of amplification that transient amplifying cell can undergo before terminal differentiation ( $\beta$ ),  
<sup>62</sup> and the relative lifespan of a terminally differentiated cell ( $\gamma$ ). While it is a simplification of reality to  
<sup>63</sup> study only these three parameters and leave out others (for example: differing proliferation rates for  
<sup>64</sup> the different cell types [7] or the differing metabolic demands of stem vs. non-stem cells [8]) rigorous  
<sup>65</sup> quantification of these parameters has been extremely difficult to pin down experimentally and so the  
<sup>66</sup> majority of the work to describe them has been *in silico*. Most germane to the loss of homeostasis is the  
<sup>67</sup> work by Enderling et al. [9] which showed the changes to the size of a mutated tissue (tumour) as they

68 varied the number of rounds of amplification of TACs. Other recent work attempting to quantify the ratio  
69 of symmetric to asymmetric division in putative glioma stem cells was presented by Lathia et al. [10], who  
70 showed that this ratio can change depending on the presence or absence of growth factors, suggesting yet  
71 another method by which a tissue can lose or maintain homeostasis: in reaction to microenvironmental  
72 change. A critical limitation of *in vivo* lineage tracing performed to date is an inability to determine the  
73 impact of microenvironmental heterogeneity on TIC symmetric division.

74 While the HM appears to be quite straight forward, there is growing evidence of complexity to be  
75 further incorporated into the model. There are likely to be differences in the extent of TIC maintenance  
76 or the ability of tumour cells to move toward a TIC state. TICs appear to reside in distinct niches  
77 suggesting there may be differences in the biology of these cells, but defining differences in TICs is  
78 limited by cell isolation and tumour initiation methods. Prospective isolation of TICs relies on surface  
79 markers, including CD133, CD151 and CD24 which can be transient in nature [11], due to modulation  
80 by the tumour microenvironment [12] or methods of isolation [13]. Characterisation of these sorted cells  
81 then requires functional assays including *in vitro* and *in vivo* limiting dilution assays [14].

82 As the importance of TICs becomes more evident as it pertains to aspects of tumour progression  
83 like heterogeneity [15], treatment resistance [16, 17], recurrence [18] and metastasis [19], the need for  
84 generalizable therapeutic strategies based on conserved motifs in these cells grows. We therefore aim  
85 to understand how the phenotypic traits discussed earlier (asymmetric division rate, allowed rounds of  
86 transient amplification and lifespan of terminally differentiated cells) and microenvironmental changes  
87 (modelled as differences in oxygen supply) effect resultant tissue growth characteristics.

88 To this end, we present a minimal spatial, hybrid-discrete/continuous mathematical model of a hi-  
89 erarchical SC-driven tissue architecture which we have used to explore the intrinsic, phenotypic, factors  
90 involved in the growth of TIC-driven tumours. We consider parameters that involve the rates of division  
91 of the cells involved in the hierarchical cascade as well as micro-environmental factors including space  
92 and competition between cell types for oxygen. We present results suggesting that there are discrete  
93 regimes in the intrinsic cellular parameter space which allow for disparate growth characteristics of the  
94 resulting tumours, specifically: TICs which form tumours that are unsustainable, TICs that are capable  
95 of forming only small colonies (spheres), and TICs that are capable of forming fully invasive tumours *in*  
96 *silico*, just as we see diversity in biological experiments (Figure 2).

## 97 Results

98 A systematic parameter exploration of the three key parameters relating to vascularisation of the domain,  
99 symmetric vs. asymmetric division ( $\alpha$ ) and progenitor division potential ( $\beta$ ) was performed. We also  
100 explored the parameter determining the lifespan of differentiated cells ( $\gamma$ ) and found that the only impact  
101 of longer lifespans is an increase in the amount of time before the simulations reach a steady state, but does  
102 not change the qualitative nature of the results. These results are summarised in Figure 3. Each of the  
103 three panels represents the results for a different degree of vascularisation (0.01, 0.05 and 0.1). A density  
104 of vascularisation of 0.05 would mean 12,500 oxygen sources in the domain. To determine the diffusion  
105 coefficient, we used the estimate of approximately 70 micrometers of effective oxygenation [20]. Each plot  
106 shows the total tissue size after 50,000 time steps as we change the proliferative potential of progenitor  
107 cells. Each of the lines shows a different ratio of symmetric vs asymmetric divisions. These results show  
108 that all these three parameters have a critical range where homeostasis is disrupted (tumourigenesis).

109 Figure 4 shows examples of the typical results produced by this model. Although the proliferation  
110 rates of all the cells remain the same, due to space constraints and the differences in  $\alpha$ , the population  
111 of TICs does not grow at the same rate as the non-stem population. Figure 4A shows an example of an  
112 unviable tissue (parameters:  $\Theta = 0.001$ ,  $\alpha = 0.3$ ,  $\beta = 50$  and  $\gamma = 1$  day) where the vascularisation does  
113 not support the potential tissue size of that TIC, resulting in an area of hypoxia affecting the region that  
114 contains the TIC. That leads to the death of the stem cell and, eventually, the rest of the cells in the tissue.  
115 Figure 4B shows a case of slightly increased symmetric division, resulting in a dynamic homeostasis where  
116 cell birth and death is balanced so that tissue size remains relatively constant - which could represent  
117 the enigmatic dormant phase [9]. Finally, figure 4C shows an example where the system never achieves  
118 true homeostasis. In this case  $\alpha$  is slightly higher when compared with the previous example, suggesting  
119 a critical value at which overgrowth occurs. Over time, the number of TICs increases, allowing for the  
120 'tumour phenotype': unconstrained growth. Although this leads to areas of hypoxia, cells survive in the  
121 periphery of the blood vessels and keep growing until they take over the entire domain. **A plot of cell**  
122 **number versus time for each of these three examples are plotted in Figure 5.**

123 Unsurprisingly, the higher the vascularisation of the domain the greater the tissue size it can support.  
124 Past a certain threshold, however, the difference becomes negligible and more remarkably, the qualitative  
125 dynamics are unchanged by any change in the microenvironment. The same effect is evident in the

126 other two parameters, the ratio of symmetric vs asymmetric division ( $\alpha$ ) of TICs and the proliferative  
127 potential of TACs ( $\beta$ ). Regardless of the vascularisation, disruption of homeostasis only occurs when  
128 the proliferative potential of TACs ( $\beta$ ) is below a maximum value of about 15. For values of symmetric  
129 division ( $\alpha$ ) above 0.3, the values for  $\beta$  in which this overgrowth occurs becomes even more restrictive  
130 with a range of approximately 10-15.

131 Interestingly, we observed a conserved decrease in overall tissue size for the highest value of symmetric  
132 division,  $\alpha = 0.5$ , when the progenitor cells were allowed only 5 divisions ( $\beta = 5$ ). We believe this  
133 phenomenon represents a situation where the tissue is not able to grow to its potential as the stem cells  
134 themselves occupy too much space, and never allow the progenitors to contribute as much as they could  
135 to the overall population. This is a supposition however, and deserves closer study. These results are  
136 summarized in Figure 3.

137 Of note as well: in no simulation did we observe the ‘tumour phenotype’ for a value of  $\alpha < 0.3$ ,  
138 suggesting something akin to a ‘phenotypic tumour suppressor’ function for this parameter. As observed  
139 biologically [10], this ratio is highly susceptible to changes in microenvironment, suggesting an extension of  
140 this minimal model to include the microenvironmental factors measured in that study. How to incorporate  
141 the changes observed in that study into a mechanistic HCA model however, is not trivial, and we reserve  
142 it for a future extension of this work. **Further, our current model exists only in two dimensions.**  
143 **While our quantitative parameters are based on experimentally derived values, the claims we**  
144 **make are largely qualitative abstractions, however, we stress that the specific quantitative**  
145 **descriptions of cell fates are likely not yet accurate and could change if this model was in**  
146 **three dimensions.**

## 147 Discussion

148 In this paper we have presented a simple **two dimensional** computational model of the HM of a TIC-  
149 driven tissue. Our results show that there are distinct regions in parameter space (that directly correlate  
150 to the intrinsic TIC phenotype space) that encode vastly different behaviour in the tissue (or tumour)  
151 arising from the TIC in question. These parameters represent different TIC phenotypes, and therefore  
152 do not represent any specific genetic mutation. In this way, we hope to generalise the intrinsic alterations  
153 which a TIC could undergo much in the same way that the hallmarks of cancer have generalised non

154 TIC-specific alterations [21]: our end goal being the identification of treatment strategies to target these  
155 phenotypes to slow or stop the progression of TIC-driven cancers.

156 Because of the difficulties in understanding TIC specific traits *in vivo*, the biological data to support  
157 these conclusions remains sparse. There have been some carefully undertaken *in vitro* experiments on  
158 single TICs in glioblastoma, a highly invasive and malignant brain tumour, which suggest that TIC  
159 specific division behaviour ( $\alpha$  in our model) is variable and changes based on environmental cues [10].  
160 Further work has shown that the other microenvironmental cues, such as acidity [14] and hypoxia [22–28]  
161 can also alter the prevalence of the stem phenotype by utilising functional markers of stemness, but the  
162 mechanism for this increase is, as of yet, imperfectly understood.

163 Our simulations do not show a significant TIC population dependence on vascular density ( $\Theta$ ), a  
164 surrogate for hypoxia, or a change in stem composition (see Supplementary Table 1), suggesting a flaw  
165 in the model. To rectify this, future iterations of this model should include direct feedback onto the  
166 cellular parameters from the microenvironment. We aim to parameterize this dependence by specific *in*  
167 *vitro* experiments designed to *quantify this effect*, rather than just elucidate its existence. Other future  
168 developments of this model should take into consideration the emerging body of work suggesting that the  
169 proportion of TICs within a tumour is directly affected by therapy and not just physiologic growth factor  
170 controls [29]. There is now evidence in several cancers to suggest that radiation increases the size of the  
171 TIC pool. Specifically, in breast cancer, it has been shown that radiation therapy induces non-stem cancer  
172 cells to de-differentiate into TICs [30]. Further, experimental studies have shown radiation increases the  
173 TIC pool in glioblastoma [31], which has often been attributed to radiation resistance associated with  
174 differences in cell survival [16]. A new study by Gao et al. [32], however, has shown *in silico* and *in vitro*  
175 that radiation can effect the symmetric to asymmetric division ratio (our intrinsic parameter  $\alpha$ ), yielding  
176 further clues about the mechanism of this TIC pool expansion.

177 Dedifferentiation due to treatment related microenvironmental factors has not yet been considered in  
178 any spatial theoretical models. Dedifferentiation due to ‘niche’ specific factors was studied by Sottoriva  
179 et al. [33], who, using an agent based model, reported findings similar to ours: that the microenvironment  
180 made no significant change to the overall tumour growth dynamics. Beyond this single spatial study, the  
181 concept of SC dedifferentiation is gaining more and more attention in conceptual theoretical treatments  
182 [34] and has been modelled with a deterministic ordinary differential equation system for a well-mixed  
183 population of cells [35].

We, as well as others, find that the HM of tissue growth does not completely capture all the necessary dynamics that characterise cancer growth - but there is still a great deal of understanding to be gained from studying this formalism. To this end, we have performed a study of the factors related to TICs driving this dynamic and have identified several key factors which promote increased growth of the resultant tumour. Motivated by Hanahan and Weinberg [21], who have simplified the myriad (epi)genetic alterations which a tumour can undergo into the hallmarks of cancer, we seek to distill the traits of TICs in a similar way. Specifically, our model suggests that the number of allowed divisions of TACs exhibits bounds outside of which tumour growth is unsustainable. This finding has been corroborated independently by recent work from Morton and colleagues [36]. Further, there is a specific balance of symmetric to asymmetric division which keeps tumours from overgrowing; almost acting as a phenotypic tumour suppressor. Indeed, changes in this ratio have been recently hypothesized to underlie the increasing stem pool in glioblastoma after irradiation [32], and could also hold a key to understanding tumour dormancy [9].

In summary, we have presented a minimal spatial Hybrid Cellular Automaton model of the HM of a TIC-driven tissue in which we have explored generalised TIC phenotypic traits and have identified several key cellular parameters which influence the overall tissue behaviour. While our model does capture a number of salient phenotypic characteristics of TICs that seem to be conserved, it fails to capture the recently observed changes in stem fraction secondary to microenvironmental perturbations. This is an indication that any computational model of a stem-hierarchical tissue, or tumour, built from this point on must not only include the physical microenvironment, but also feedback from the microenvironment onto the specific cellular parameters encoded in the HM.

Therefore, this endeavour has identified the crucial point that the microenvironment must effect the behaviour of the cells within the HM, and also several conserved phenotypic hallmarks, which could be the result of any number of (epi)genetic alterations or microenvironmental perturbations. By focussing on mechanisms important for the HM of stem-cell driven tumour growth, we are seeking to identify common phenotypes which could be targeted in a variety of solid tumours in which TICs promote tumour maintenance - thereby reducing the number of therapeutic targets to a more tractable set. Only with this sort of distillation of the biological complexity inherent to cancer initiation (and indeed progression) can we hope to make progress against this disease.

## 213 Materials and Methods

214 Our model is based on a hybrid, discrete-continuous cellular automaton model (HCA) of a hierarchically  
215 structured tissue. HCA models have been used to study cancer progression and evolutionary dynamics  
216 since they can integrate biological parameters and produce predictions affecting different spatial and time  
217 scales [15, 33, 37–40]. As shown in figure 6C, cells are modelled in a discrete fashion on a 500x500 2-D  
218 lattice. This comprises approximately  $1\text{cm}^2$  where we assume a cell diameter of 20 micrometers [41].  
219 The domain has periodic boundary conditions but the simulations are stopped when a cell reaches one  
220 of the boundaries. Every time step, cells are iterated in a random fashion as to avoid any bias in the  
221 way that cells are chosen. Figure 6A shows that, although all cells are assumed to have the same size  
222 and shape, they can only be one of three different phenotypes: TICs capable of infinite divisions, TACs  
223 which are capable of division into two daughters for a certain number ( $\beta$ ) of generations, and TDs which  
224 cannot divide but live and consume nutrients for a specified lifetime ( $\gamma$ ). Modes of division for TICs  
225 include asymmetric division (with probability  $1 - \alpha$ ), which is division into one TIC daughter and one  
226 TAC daughter and symmetric division, which is division into two TIC daughters (probability  $\alpha$ ).

227 The continuous portion of this model is made up of the distribution and consumption of nutrients (in  
228 this case modelled only as oxygen). Vessels, which are modelled as point sources and take up one lattice  
229 point ( $V_{i,j}$  in Equation 1), are placed randomly throughout the grid at the initiation of a given simulation,  
230 in a specified density ( $\Theta$ ). Each of these vessels supplies oxygen at a constant rate ( $\lambda$ ) which then diffuses  
231 into the surrounding tissue. The diffusion speed/distance is described by Equation 1, where  $O(x, y, t)$  is  
232 the concentration of oxygen at a given time ( $t$ ), and place ( $x, y$ ),  $D_O$  is the diffusion coefficient of oxygen,  
233  $\lambda$  is the rate of oxygen production from a blood vessel,  $\mu_s$ ,  $\mu_p$ , and  $\mu_t$  are the rates at which TIC, TAC  
234 and TD cells consume oxygen. The difference in time scales that govern the diffusion of nutrients and  
235 that at which cells operate is managed by updating the continuous part of the model 100 times per time  
236 step. During each update the oxygen tension in a given grid point is updated with the values of the  
237 surrounding cells using a von Neumann neighbourhood modulated by the diffusion rate ( $D_O$ ).

$$\frac{\partial O(x, y, t)}{\partial t} = D_O \nabla^2 O(x, y, t) + \lambda V_{x,y} - \mu_S S_{x,y} - \mu_P P_{x,y} - \mu_T T_{x,y} \quad (1)$$

238 Any simulation performed by this model can be characterised by the parameters found in Figure 7.  
239 The most relevant parameters for the question we are trying to address are the following:

240 • Symmetric/asymmetric division rate of stem cells ( $\alpha$ )

241 • Vascular density of the tissue ( $\Theta$ )

242 • Number of allowed divisions of TACs ( $\beta$ )

243 • Lifespan of TDs ( $\gamma$ )

244 In each case, as can be seen in figure 6, a simulation is seeded with one TIC with a given set of intrinsic  
245 parameters ( $\alpha, \beta, \gamma$ ) governing its and its progeny's behaviour, which is placed in the centre of the  
246 computational domain. The domain is initialised with as many randomly placed oxygen source points  
247 (vasculature) as described by the vascular density parameter ( $\Theta$ ).

## 248 Acknowledgments

## 249 References

- 250 1. Singh SK, Hawkins C, Clarke ID, Squire JA, Bayani J, et al. (2004) Identification of human brain  
251 tumour initiating cells. *Nature* 432: 396-401.
- 252 2. Al-Hajj M, Wicha MS, Benito-Hernandez A, Morrison SJ, Clarke MF (2003) Prospective identification  
253 of tumorigenic breast cancer cells. *Proc Natl Acad Sci U S A* 100: 3983-8.
- 254 3. Ricci-Vitiani L, Lombardi DG, Pilozzi E, Biffoni M, Todaro M, et al. (2007) Identification and  
255 expansion of human colon-cancer-initiating cells. *Nature* 445: 111-5.
- 256 4. Diehn M, Cho RW, Clarke MF (2009) Therapeutic implications of the cancer stem cell hypothesis.  
257 *Semin Radiat Oncol* 19: 78-86.
- 258 5. Morrison SJ, Kimble J (2006) Asymmetric and symmetric stem-cell divisions in development and  
259 cancer. *Nature* 441: 1068-74.
- 260 6. Reya T, Morrison SJ, Clarke MF, Weissman IL (2001) Stem cells, cancer, and cancer stem cells.  
261 *Nature* 414: 105-11.
- 262 7. Werner B, Dingli D, Lenaerts T, Pacheco JM, Traulsen A (2011) Dynamics of mutant cells in  
263 hierarchical organized tissues. *PLoS Comput Biol* 7: e1002290.
- 264 8. Vlashi E, Lagadec C, Vergnes L, Matsutani T, Masui K, et al. (2011) Metabolic state of glioma  
265 stem cells and nontumorigenic cells. *Proc Natl Acad Sci U S A* 108: 16062-7.
- 266 9. Enderling H, Anderson ARA, Chaplain MAJ, Beheshti A, Hlatky L, et al. (2009) Paradoxical  
267 dependencies of tumor dormancy and progression on basic cell kinetics. *Cancer Res* 69: 8814-21.
- 268 10. Lathia JD, Hitomi M, Gallagher J, Gadani SP, Adkins J, et al. (2011) Distribution of cd133 reveals  
269 glioma stem cells self-renew through symmetric and asymmetric cell divisions. *Cell Death Dis* 2:  
270 e200.

- 271 11. Gupta PB, Fillmore CM, Jiang G, Shapira SD, Tao K, et al. (2011) Stochastic state transitions  
272 give rise to phenotypic equilibrium in populations of cancer cells. *Cell* 146: 633-44.
- 273 12. Flavahan WA, Wu Q, Hitomi M, Rahim N, Kim Y, et al. (2013) Brain tumor initiating cells adapt  
274 to restricted nutrition through preferential glucose uptake. *Nat Neurosci* 16: 1373-82.
- 275 13. Brescia P, Richichi C, Pelicci G (2012) Current strategies for identification of glioma stem cells:  
276 adequate or unsatisfactory? *J Oncol* 2012: 376894.
- 277 14. Hjelmeland AB, Wu Q, Heddleston JM, Choudhary GS, MacSwords J, et al. (2011) Acidic stress  
278 promotes a glioma stem cell phenotype. *Cell Death Differ* 18: 829-40.
- 279 15. Sottoriva A, Verhoeff JJC, Borovski T, McWeeney SK, Naumov L, et al. (2010) Cancer stem cell  
280 tumor model reveals invasive morphology and increased phenotypical heterogeneity. *Cancer Res*  
281 70: 46-56.
- 282 16. Bao S, Wu Q, McLendon RE, Hao Y, Shi Q, et al. (2006) Glioma stem cells promote radioresistance  
283 by preferential activation of the dna damage response. *Nature* 444: 756-60.
- 284 17. Chen J, Li Y, Yu TS, McKay RM, Burns DK, et al. (2012) A restricted cell population propagates  
285 glioblastoma growth after chemotherapy. *Nature* 488: 522-6.
- 286 18. Dingli D, Michor F (2006) Successful therapy must eradicate cancer stem cells. *Stem Cells* 24:  
287 2603-10.
- 288 19. Pang R, Law WL, Chu ACY, Poon JT, Lam CSC, et al. (2010) A subpopulation of cd26+ cancer  
289 stem cells with metastatic capacity in human colorectal cancer. *Cell Stem Cell* 6: 603-15.
- 290 20. Hall EJ, Giaccia AJ (2012) Radiobiology for the radiologist. Philadelphia: Wolters Kluwer  
291 Health/Lippincott Williams and Wilkins, 7th ed edition.
- 292 21. Hanahan D, Weinberg RA (2011) Hallmarks of cancer: the next generation. *Cell* 144: 646-74.
- 293 22. Heddleston JM, Li Z, McLendon RE, Hjelmeland AB, Rich JN (2009) The hypoxic microenvironment  
294 maintains glioblastoma stem cells and promotes reprogramming towards a cancer stem cell  
295 phenotype. *Cell Cycle* 8: 3274-84.
- 296 23. Li Z, Bao S, Wu Q, Wang H, Eyler C, et al. (2009) Hypoxia-inducible factors regulate tumorigenic  
297 capacity of glioma stem cells. *Cancer Cell* 15: 501-13.
- 298 24. Seidel S, Garvalov BK, Wirta V, von Stechow L, Schänzer A, et al. (2010) A hypoxic niche regulates  
299 glioblastoma stem cells through hypoxia inducible factor 2 alpha. *Brain* 133: 983-95.
- 300 25. Bar EE, Lin A, Mahairaki V, Matsui W, Eberhart CG (2010) Hypoxia increases the expression  
301 of stem-cell markers and promotes clonogenicity in glioblastoma neurospheres. *Am J Pathol* 177:  
302 1491-502.
- 303 26. Soeda A, Park M, Lee D, Mintz A, Androutsellis-Theotokis A, et al. (2009) Hypoxia promotes  
304 expansion of the cd133-positive glioma stem cells through activation of hif-1alpha. *Oncogene* 28:  
305 3949-59.
- 306 27. Mathieu J, Zhang Z, Zhou W, Wang AJ, Heddleston JM, et al. (2011) Hif induces human embryonic  
307 stem cell markers in cancer cells. *Cancer Res* 71: 4640-52.

- 308 28. Kolenda J, Jensen SS, Aaberg-Jessen C, Christensen K, Andersen C, et al. (2011) Effects of hypoxia  
309 on expression of a panel of stem cell and chemoresistance markers in glioblastoma-derived spheroids.  
310 *J Neurooncol* 103: 43-58.
- 311 29. Vermeulen L, De Sousa e Melo F, van der Heijden M, Cameron K, de Jong JH, et al. (2010) Wnt  
312 activity defines colon cancer stem cells and is regulated by the microenvironment. *Nat Cell Biol*  
313 12: 468-76.
- 314 30. Lagadec C, Vlashi E, Della Donna L, Dekmezian C, Pajonk F (2012) Radiation-induced repro-  
315 gramming of breast cancer cells. *Stem Cells* 30: 833-44.
- 316 31. Tamura K, Aoyagi M, Wakimoto H, Ando N, Narai T, et al. (2010) Accumulation of cd133-positive  
317 glioma cells after high-dose irradiation by gamma knife surgery plus external beam radiation. *J*  
318 *Neurosurg* 113: 310-8.
- 319 32. Gao X, McDonald JT, Hlatky L, Enderling H (2013) Acute and fractionated irradiation differen-  
320 tially modulate glioma stem cell division kinetics. *Cancer Res* 73: 1481-90.
- 321 33. Sottoriva A, Sloot PMA, Medema JP, Vermeulen L (2010) Exploring cancer stem cell niche directed  
322 tumor growth. *Cell Cycle* 9: 1472-9.
- 323 34. Vermeulen L, de Sousa e Melo F, Richel DJ, Medema JP (2012) The developing cancer stem-cell  
324 model: clinical challenges and opportunities. *Lancet Oncol* 13: e83-9.
- 325 35. Leder K, Holland EC, Michor F (2010) The therapeutic implications of plasticity of the cancer  
326 stem cell phenotype. *PLoS One* 5: e14366.
- 327 36. Morton CI, Hlatky L, Hahnfeldt P, Enderling H (2011) Non-stem cancer cell kinetics modulate  
328 solid tumor progression. *Theor Biol Med Model* 8: 48.
- 329 37. Anderson ARA (2005) A hybrid mathematical model of solid tumour invasion: the importance of  
330 cell adhesion. *Math Med Biol* 22: 163-86.
- 331 38. Anderson ARA, Hassanein M, Branch KM, Lu J, Lobdell NA, et al. (2009) Microenvironmental  
332 independence associated with tumor progression. *Cancer Res* 69: 8797-806.
- 333 39. Anderson ARA, Weaver AM, Cummings PT, Quaranta V (2006) Tumor morphology and pheno-  
334 typic evolution driven by selective pressure from the microenvironment. *Cell* 127: 905-15.
- 335 40. Basanta D, Strand DW, Lukner RB, Franco OE, Cliffel DE, et al. (2009) The role of transforming  
336 growth factor-beta-mediated tumor-stroma interactions in prostate cancer progression: an integra-  
337 tive approach. *Cancer Res* 69: 7111-20.
- 338 41. Melicow MM (1982) The three steps to cancer: a new concept of cancerogenesis. *J Theor Biol* 94:  
339 471-511.

<sup>340</sup> **Figure Legends**

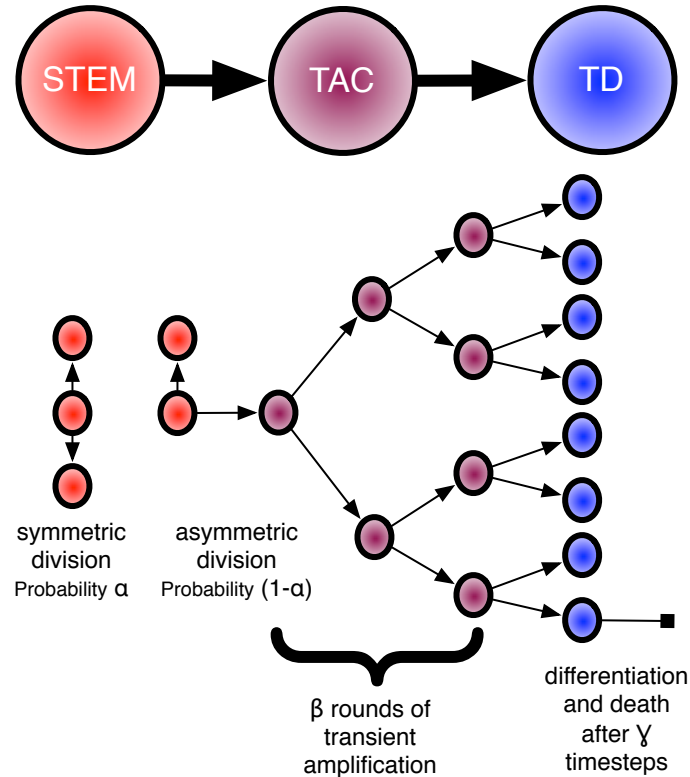


**Figure 1. Cartoon representing the hierarchical model of stem-cell driven tissues.** In this formulation, each stem can undergo two types of division, either symmetric (with probability  $\alpha$ ) or asymmetric (with probability  $1 - \alpha$ ). Each subsequently generated transient amplifying cell (TAC) can then undergo a certain number ( $\beta$ ) of rounds of amplification before differentiating into a terminally differentiated cell (TD) which will live for a certain amount of time before dying ( $\gamma$  timesteps). It is these three parameters, which we assume are intrinsic to a given stem cell, which we explore in this paper.

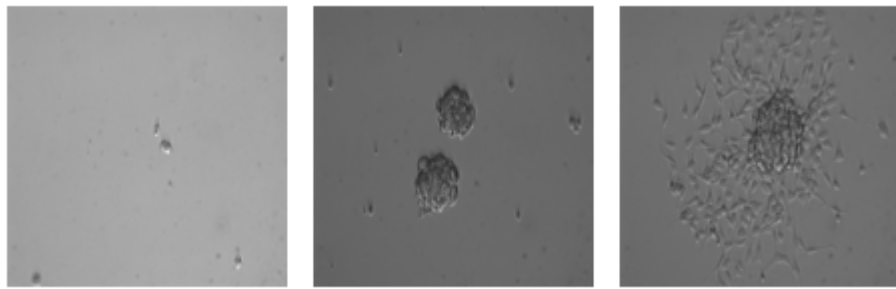


**Figure 2. Differential phenotypes in cultures enriched for brain tumour initiating cells.**  
Bright field images of CD133+ patient derived glioblastoma cell lines cultured in Neurobasal supplemented with EGF, FGF and B27, exhibiting striking phenotypic variability. These differences highlight the heterogeneity present even in a highly controlled static environment between cells that are putatively the same.

<sup>341</sup> **Tables**

**Table 1. Supplementary Information.** Raw stem and total cell numbers from several runs of the CA with varying parameter combinations.

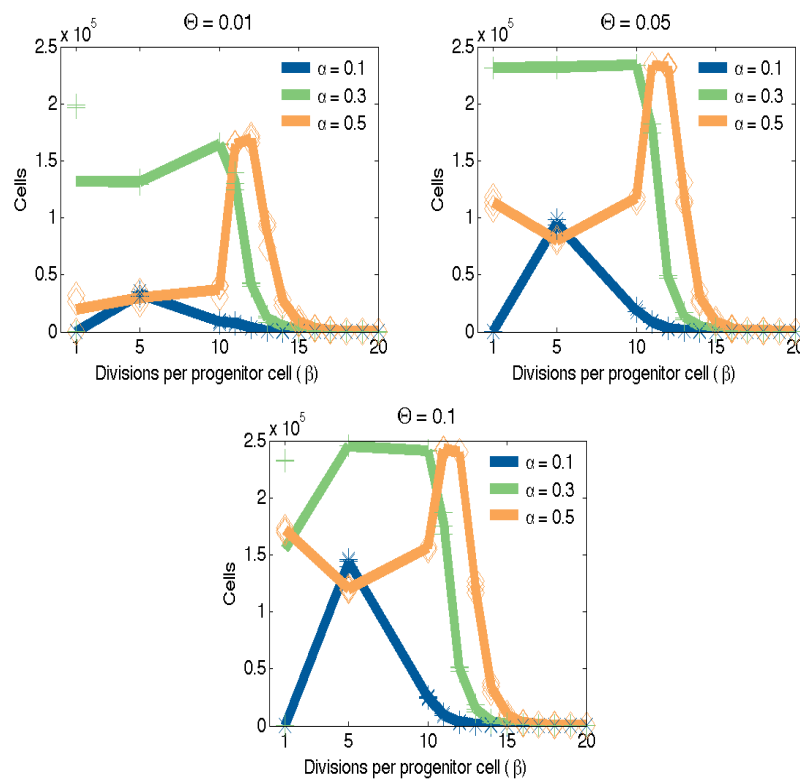


**Figure 3.** Size of tissues vs. progenitor proliferative potential achieved by simulations using different levels of vascularisation and ratios of symmetric vs asymmetric divisions. Lines represent averages for each of the three realisations in each scenario. (Left). Low vascularisation density of 0.01 (Centre) Normal vascularisation density of 0.05 (Right) High vascularisation density of 0.1. In each of these cases, the maximum tissue size will depend on the right combination of  $\alpha$  and  $\beta$ .

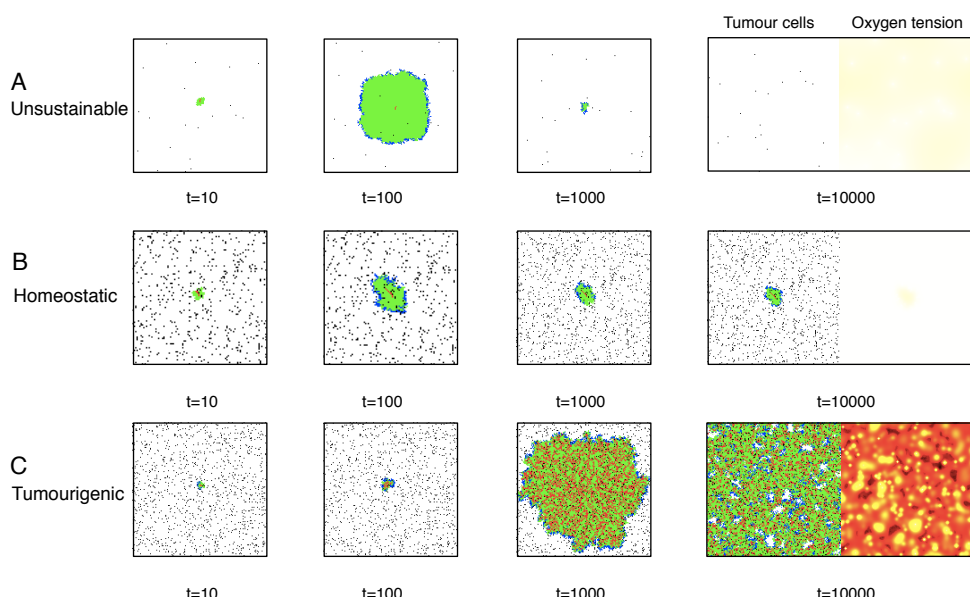


**Figure 4. Three different examples of simulations resulting from the computational model. Each simulation represents one of the typical outcomes.** Each begins with a single TIC seeded in the middle of the computational domain. In each situation the phenotype parameters are slightly different, resulting in (A) An unsustainable tissue (parameters:  $\Theta = 0.001$ ,  $\alpha = 0.3$ ,  $\beta = 50$  and  $\gamma = 1$  day), (B) A homeostatic tissue where the balance of stem cell self renewal and progenitor proliferation leads to a tissue whose overall size remains relatively constant over time, possibly representing a dormant tumor (parameters:  $\Theta = 0.05$ ,  $\alpha = 0.3$ ,  $\beta = 15$  and  $\gamma = 1$  day) and, (C) Neoplastic-like tissue where the tissue overgrows the computational domain (parameters:  $\Theta = 0.05$ ,  $\alpha = 0.3$ ,  $\beta = 5$  and  $\gamma = 1$  day). **On the right of the final time point, we have shown an example of the oxygen tension in the computational domain.** n.b. these images are zoomed in to illustrate detail and do not represent the entire computational domain.

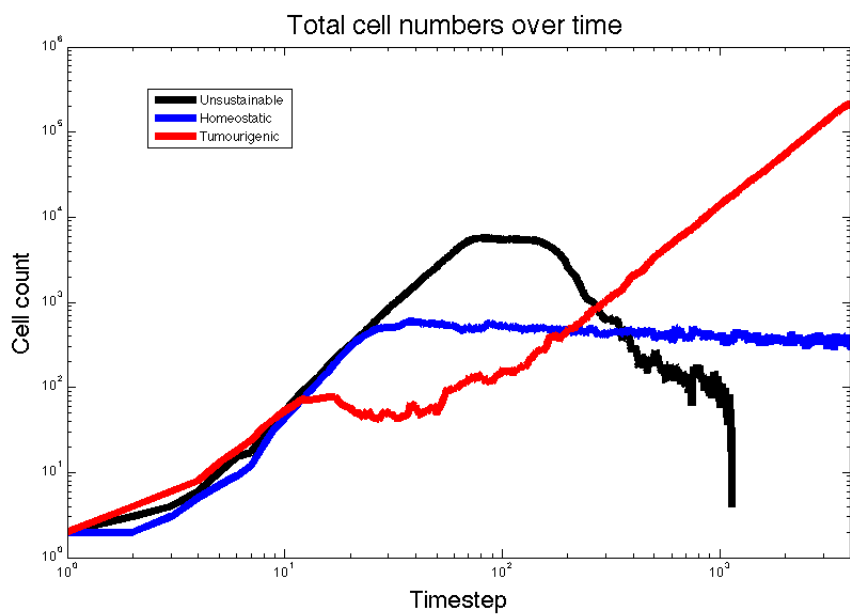


**Figure 5.** The three qualitatively different tissue scale phenotypes plotted as cell numbers over time for the example simulations in figure 4. The black trace, representing the unsustainable simulation, grows quickly though never expands its stem population and then outstrips the available oxygen and collapses. The blue trace, representing the Homeostatic simulation, reaches a critical size and then maintains a steady birth-death balance. The red trace, representing the tumorigenic simulation, settles into an effectively linear trace on this log-log plot, suggesting power law growth.

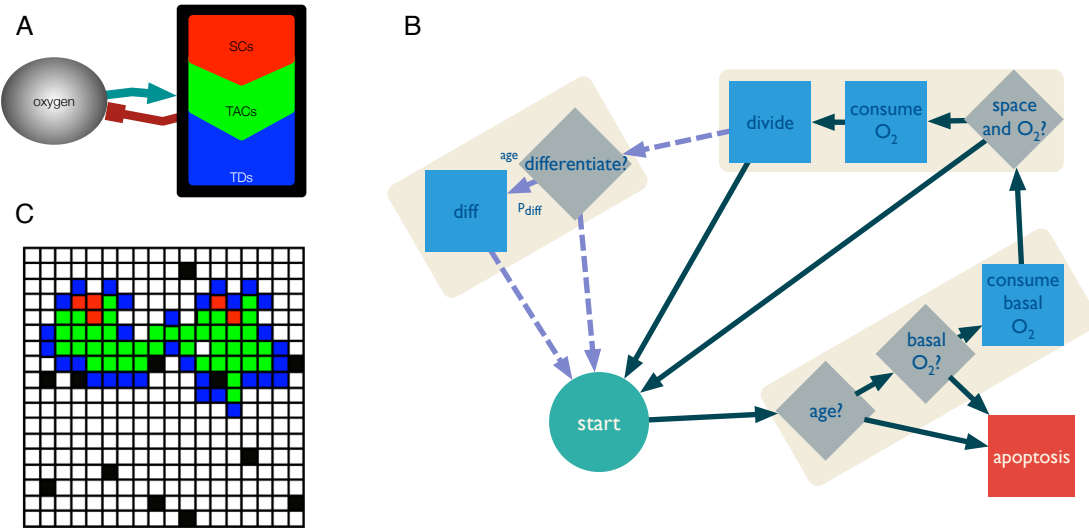


**Figure 6. Computational model description.** (A) The model includes three different cell types: **stem, progenitor and differentiated**. All cell types interact with the microenvironment in the form of oxygen tension. (B) The behaviour of each cell type is captured by a flowchart. The last segment with discontinuous arrows represents behaviour that is specific to the stem cells. (C) The cells are represented as agents inhabiting points in a 2D space with 500x500 grid points. Stem cells are represented as red points, progenitor as green and fully differentiated as blue. The vasculature is represented as oxygen source points in black.

Parameter	value
Do (Oxygen diffusion)	0.001728
$\lambda$ (Rate of Oxygen production)	1
$\mu_s, \mu_p, \mu_T$	0.0001
$\alpha$ (Ratio of SC symmetric division)	0.1, 0.3, 0.5
$\beta$ (TAC proliferative potential)	1,5,10,11,12,13,14,15,16,1 7,18,19,20,50,70,100
$\gamma$ (Differentiated cell lifespan)	1
$\Theta$ (Vascularisation)	0.001, 0.01, 0.05, 0.1, 0.5

**Figure 7. Model parameters.**